

Kitaev quasiparticles in a proximate spin liquid: A many-body localization perspective

Aman Kumar and Vikram Tripathi

*Department of Theoretical Physics, Tata Institute of Fundamental Research,
Homi Bhabha Road, Navy Nagar, Mumbai 400005, India*

(Dated: December 21, 2024)

We study the stability of Kitaev quasiparticles in the presence of a perturbing Heisenberg interaction as a Fock space localization phenomenon. We identify parameter regimes where Kitaev states are localized, fractal or delocalized in the Fock space of exact eigenstates, with delocalization implying quasiparticle instability. Finite temperature calculations show that a vison gap, and a nonzero plaquette Wilson loop at low temperatures, both characteristic of the deconfined Kitaev spin liquid phase, persist far into the neighboring proximate spin liquid phase that has a concomitant stripy spin-density wave order. Remarkably, Kitaev quasiparticle excitations are stable at low-energy states over a significant parameter space in the stripy phase.

The honeycomb Kitaev model describes an integrable Z_2 quantum spin liquid exhibiting the spin-fractionization phenomenon. The Kitaev quasiparticles consist of gapped Z_2 plaquette fluxes (visons) and deconfined Majorana fermions (spinons) [1]. Considerable theoretical [2–24] and experimental [25–42] debate surrounds the question of Kitaev quasiparticle effects in the presence of competing spin-interactions, since in the commonly studied Kitaev materials[43–47], the ground state is magnetically ordered. Experimental observations such as the incoherent features in inelastic neutron scattering [3, 43] and the broad peak in THz spectroscopy [27, 41] at higher energies, as well as thermal conductivity[28, 48], thermal Hall response[42], and high field torque response [48, 49] have been interpreted in both ways as evidence of Kitaev physics [4, 25, 42, 49, 50] as well as magnon interaction [3] and other anisotropy effects [51]. This motivates us to pose a basic question independent of material specific details: can many-body excitations of a Kitaev model subjected to a Heisenberg perturbation resemble the quasiparticles of a Kitaev model over a range of energies even as the ground state may have spin density wave order?

Here we study the stability of Kitaev quasiparticles for a simple ($J - K$) model, consisting of ferromagnetic (FM) Kitaev (K) and antiferromagnetic (AFM) Heisenberg (J) interactions, using recently developed exact diagonalization methods, namely FEAST [52] and Krylov-Schur[53] algorithms for systems of up to $N = 24$ spins. The FEAST [52] eigensolver algorithm is based on a contour intergation projection technique. It allows evaluation of eigenstates within an arbitrary user-specified eigenvalue range, and is able to handle degeneracies. Computing a large number of states is necessary not only to establish Fock space delocalization but also for the study of specific signatures of the Kitaev spin liquid such as the vison gap that exists only at higher energies, and would not be readily accessible from an analysis of the ground state properties such as that usually computed using Lanczos or density matrix renormalization group methods [54]. For the higher system sizes ($N = 20 - 24$), because of large memory requirements of FEAST, we instead use the Krylov-Schur algorithm that gives us significant numbers

of eigenstates, including degeneracies, near the extreme ends of the spectrum ($\sim 2 \times 10^3$ for $N = 24$), and works better than Lanczos algorithms.

The ground state of our model is known [5, 20] to be a paramagnetic Kitaev spin liquid (KSL) in the parameter range $0 \leq J/K \lesssim 0.12$, exhibiting a stripy AFM order for $0.12 \lesssim J/K \lesssim 0.75$, and Néel AFM order for larger J/K . There is also a special point, $J/K = 0.5$, where stripy AFM order peaks, and where, upon a sublattice transformation [5], the $J - K$ model in the transformed basis maps exactly to an isotropic Heisenberg ferromagnet implying the stripy AFM is an exact ground state at this point. The regime $0.12 \lesssim J/K \lesssim 0.5$ is our proximate spin liquid phase (PSL) where the ground state shows magnetic order but the proximity to the KSL phase implies significant Kitaev correlations.

We find that low-energy states over a significant range of the interaction parameter in the PSL corresponding to $0.12 \lesssim J/K \lesssim 0.5$, Kitaev quasiparticles corresponding to the $J/K = 0$ limit are stable, and in the vicinity of the KSL-PSL phase boundary, better describe the exact eigenstates than the stripy wavefunctions corresponding to $J/K = 0.5$. On the average, states with comparable energy densities have comparable stabilities. We obtain energy density windows where Kitaev quasiparticles are stable for $J/K \gtrsim 0.12$. At high enough energy densities comparable to the stripy AFM ordering scale, the PSL states resemble neither Kitaev nor stripy AFM quasiparticles. Our finite temperature calculations show the presence of a vison gap, and at low temperatures, a nonzero value of the Kitaev plaquette fluxes, both signatures of the deconfined KSL phase, persisting in the PSL all the way to $J/K = 0.5$, despite the simultaneous presence of stripy AFM order.

The problem of quasiparticle stability in interacting systems has a deep connection to the many-body localization (MBL) phenomenon [55]. To see this, we represent individual Kitaev eigenstates as linear superpositions of the exact eigenstates of the ($J - K$) model in the parameter space $J/K \in [0, \infty]$. In the basis of exact eigenstates, the scaling of the support size ξ of the Kitaev states with the dimensionality $D = 2^N$ of the Fock space in accordance with the law $\xi \sim D$ implies a

fully many-body delocalized state or a decaying quasiparticle, while $\xi \sim D^0$ corresponds to a localized state where the quasiparticle does not decay. A third possibility, $\xi \sim 2^{cN} = D^c$, with $c < 1$, represents a fractal delocalized state and still corresponds to a long-lived quasiparticle excitation since $\xi/D \rightarrow 0$ as $D \rightarrow \infty$.

We begin our analysis with the following nearest-neighbour $J - K$ model:

$$H = -K \sum_{\langle ij \rangle, \gamma} \sigma_i^\gamma \sigma_j^\gamma + J \sum_{\langle ij \rangle} \boldsymbol{\sigma}_i \cdot \boldsymbol{\sigma}_j, \quad (1)$$

where $K, J > 0$, $\gamma = x, y, z$ labels an axis in spin space and a bond direction of the honeycomb lattice and σ_i^γ represent Pauli spin matrices at the site labeled i . We consider clusters with (even) number N of spins ranging from 10 to 24, and subjected to periodic boundary conditions.

We use the FEAST eigensolver algorithm[52] to compute the large numbers of eigenvectors in arbitrarily specified energy ranges for different values of the ratio J/K for N up to 18 spins. Unlike the usual projection methods such as Lanczos and Jacobi-Davidson that are based on the Krylov subspaces, the FEAST algorithm implements projection using the contour integration based projector,

$$\frac{1}{2\pi i} \oint_C \frac{dE}{EI - H} |v\rangle = \sum_{n \in C} \langle n|v\rangle |n\rangle, \quad (2)$$

where $|v\rangle$ is in general some random vector defined on the entire Fock space of dimension $D = 2^N$, and $\{|n\rangle\}$ are the eigenvectors corresponding to, say, m eigenvalues lying within the user-defined contour C . By choosing a number $p \geq m$, of these random vectors (in general linearly-independent), we end up with a set of m linearly-independent vectors spanning the eigenspace enclosed in C . Among the advantages this method offers are suitability for parallelization and the ability to obtain large numbers of eigenvectors in user-specified energy ranges, including degeneracies. For $N = 20$ to 24, memory requirements restrict our usage of FEAST, and for that we employed the Krylov-Schur algorithm[53] which yields a significant number of levels (around 1500 for $N = 24$ on our machine) reckoned from the extreme ends of the excitation spectrum. While this does not yield information about states in the middle of the spectrum, it is sufficient to demonstrate Fock space localization of Kitaev states in the $J - K$ model.

To study the resemblance of a given Kitaev state $|\alpha_k\rangle$ with the exact eigenstates $|\psi_i\rangle$ of the $J - K$ model, we expand it as a linear superposition,

$$|\alpha_k\rangle = \sum_{i=1}^D a_{ki} |\psi_i\rangle, \quad (3)$$

and obtain the inverse participation ratio (IPR),

$$P_k = \sum_{i=1}^D |a_{ki}|^4. \quad (4)$$

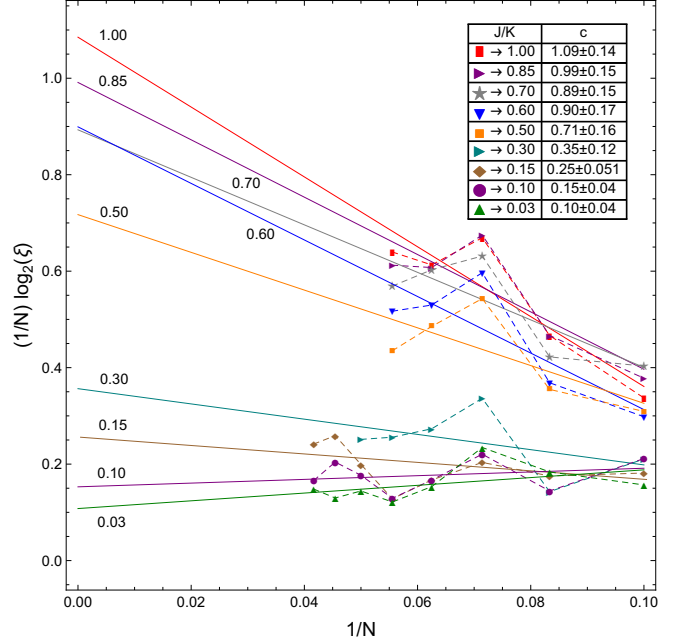


Figure 1. Plot describing finite size scaling of the support size, ξ , of the lowest two-vortex Kitaev state (a low-energy excitation) in the Fock space of exact states of the $J - K$ model for $0.03 \leq J/K \leq 1$ and up to $N = 24$ spins. The fits (solid lines) are to a law of the form $\xi = f2^{cN}$. Lines with negative (positive) slopes correspond to many-body delocalized (localized) phases. The localized to fractal transition for this state occurs at the Kitaev-stripy AFM phase boundary, $J/K \approx 0.12$ and fractal to delocalized at the peak of the stripy order, $J/K = 0.5$. The numbers on the solid lines indicate the value of J/K .

The support size for the state $|\alpha_k\rangle$ is then $\xi_k = 1/P_k$. In practice, only the states contributing significantly to the IPR need to be computed - these states have relatively large overlaps a_{ki} . Calculation of the entire eigensystem for smaller N gives an estimate of the energy window(s) where most of the support is present, and this informs our choice of energy range in larger system sizes for which FEAST is used. As our goal is to understand whether the exact eigenstates for a given J/K resemble the Kitaev quasiparticles or the the stripy SDW excitations, we also perform the same analysis for the eigenstates corresponding to $J/K = 0.5$.

Fig. 1 shows a plot of $(1/N) \log_2 \xi$ vs $1/N$ for a low-lying two-flux Kitaev state for different values of J/K , and N up to 24, together with linear fits. In the unperturbed Kitaev model, this two-flux state has an energy close to the ground state. In the delocalized or fractal phases, where $\xi \sim 2^{cN}$, the slope $(-\ln_2(1/f))$ is negative, while in the MBL phase where the support scales sub-exponentially, the slope is positive. The Heisenberg interaction does not in general connect all pairs of Kitaev states even in the delocalized phases; thus $f < 1$. The intercept gives us the exponent c in the delocalized and fractal phases. We find that for small perturbations,

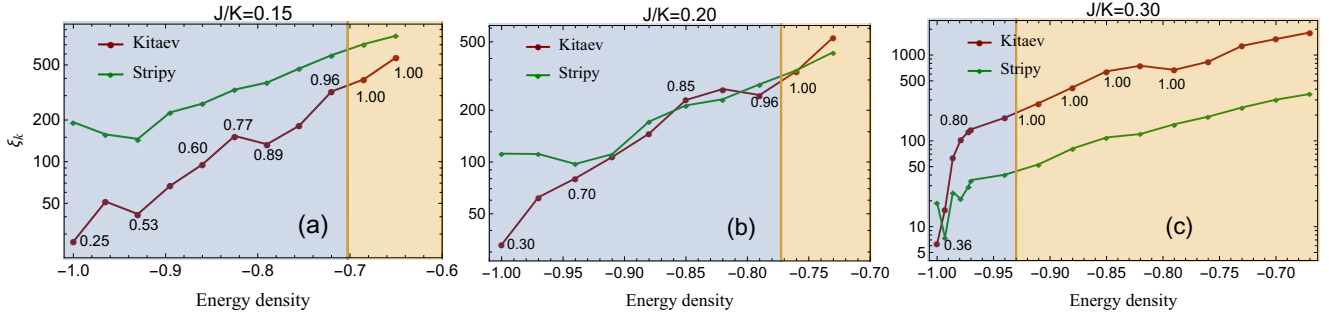


Figure 2. Calculated support sizes ξ for the Kitaev and stripy SDW states (corresponding to $J/K = 0$ and $J/K = 0.5$ respectively) in the Fock space of exact eigenstates of the $J - K$ model for three different points in the proximate spin liquid (PSL) phase. The energy density, i.e., the energy per site, has been expressed in dimensionless units by normalizing with respect to the ground state energy. The blue shaded regions indicate Kitaev states showing fractal finite size scaling, $\xi \sim 2^{cN}$, $c < 1$, (stable Kitaev quasiparticles) while the yellow shaded region corresponds to fully delocalized (unstable) Kitaev states. The numbers on the curves show the values of the exponent c for the Kitaev states obtained from finite-size scaling at a given energy density. The values of c corresponding to stripy states (not shown) were found to be respectively larger for $J/K = 0.15$, comparable for $J/K = 0.2$, and smaller for $J/K = 0.3$. The exact eigenstates in the PSL are more Kitaev-like at low energy densities and smaller values of J/K .

$J/K \lesssim 0.12$, the support ξ is small, shows fluctuations as a function of N , but does not increase exponentially at least up to $N = 24$. For $0.12 \lesssim J/K \lesssim 0.5$, the increase is exponential, $\xi \sim f2^{cN}$, with the exponent $c < 0.71 \pm 0.16$, signifying a fractal delocalized phase. Beyond $J/K = 0.5$, the exponent sharply increases, within numerical accuracy, to $c \approx 1$, and remains near this value for larger J/K . This regime corresponds to fully delocalized low-lying Kitaev states. These MBL transitions respectively occur in the vicinity of the Kitaev-stripy AFM transition point ($J/K \approx 0.12$) and the special point $J/K = 0.5$ where the stripy SDW order peaks. We also studied the scaling behavior of the entanglement entropy S_k ,

$$S_k = - \sum_{i=1}^D |a_{ki}|^2 \log_2 |a_{ki}|^2, \quad (5)$$

and found it in agreement (see Appendix) with conclusions drawn from the scaling of ξ . We conclude that for $J/K \gtrsim 0.5$, this two-flux Kitaev state is completely delocalized in the Fock space ($\xi \approx fD$) and consequently decays, while for smaller J/K , it is either fractal or many-body localized and consequently infinitely long-lived.

In Fig. 2 we show the support sizes for the Kitaev ($J/K = 0$) and stripy AFM ($J/K = 0.5$) states in the Fock space of the exact eigenstates of the $J - K$ model as a function of the normalized energy density for three representative values of J/K in the PSL phase for an 18-site cluster [56]. The choice of normalized energy density for characterizing the support sizes of the quasiparticles is based on our empirical observation that states with comparable energies have comparable support sizes (see Appendix). For $J/K = 0.15$, in the PSL phase close to the KSL phase boundary (Fig. 2(a)), the Kitaev states clearly have smaller support sizes compared to stripy SDW. Furthermore, we have performed a finite-size scal-

ing analysis at fixed energy density to determine the nature of Fock space localization of the states. The blue shaded region refers to the fractal phase of Kitaev states, beyond which the fully delocalized phase appears where Kitaev quasiparticles decay. The numbers on the Kitaev curve denote the calculated scaling exponent c . Finite-size scaling analysis of the support of stripy SDW states for $J/K = 0.15$ shows that they delocalize at lower energy densities than the corresponding Kitaev states, and have larger values of c (not shown in the Figure). The case $J/K = 0.2$ (Fig. 2(b)) is deeper in the PSL phase. At the lowest energy densities, the Kitaev states have still have smaller support sizes than stripy SDW, and finite size scaling analysis shows that they are also more localized. Beyond the lowest energy densities, the Kitaev and stripy SDW states show similar scaling behavior, and the phase boundaries separating fractal and completely delocalized phases occur at comparable energy densities for the two. Further away (2(c)), for $J/K = 0.3$ that is also in the PSL phase, there is only a very small region of low energy density where Kitaev states have a smaller support than stripy SDW, and are stable. For this value of J/K , the stripy SDW states continue to show fractal scaling (stability) to much higher energy densities (~ -0.7). We conclude that in the PSL phase, the exact eigenstates may be approximated as Kitaev states only for low energy densities, and beyond a sufficiently high energy density that depends on J/K , both Kitaev and stripy SDW descriptions are not appropriate.

Figure 3 shows the phase diagram of the Kitaev states according to their finite size scaling behavior in the J/K vs. energy density plane. Low energy Kitaev states are clearly more robust against delocalization compared to the high energy states by a Heisenberg perturbation. As one approaches the middle of the spectrum, where the energy density is zero, Kitaev states get delocalized even by small perturbations. We also found that this behav-

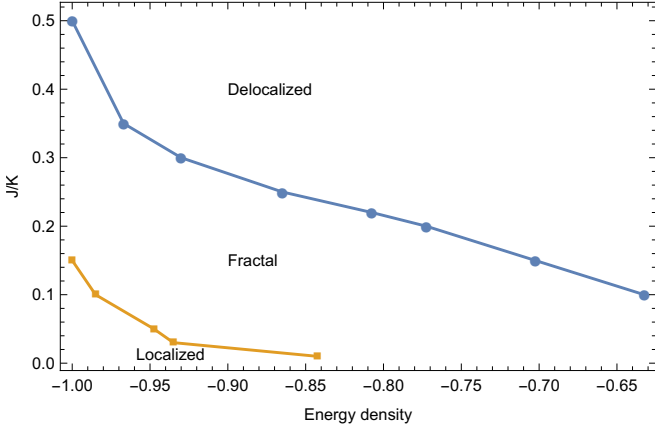


Figure 3. Phase diagram showing different finite size scaling (up to 24 sites) regimes of Kitaev quasiparticle states as a function of J/K and energy density. Kitaev quasiparticles are stable in the localized and fractal scaling regimes, and unstable in the delocalized regime. The PSL phase corresponds to $J/K \gtrsim 0.12$. Kitaev states are not localized in the PSL phase but are nevertheless stable over a significant low energy range where they show fractal scaling. States corresponding to high energy density states are delocalized and cannot be regarded as Kitaev-like.

ior is mirrored on the side of positive energy densities (not shown in the Figure) - the highest positive energy excited states show a similar behavior as those close to the ground state.

Figure 4 shows the temperature (T) vs. J phase diagram obtained from a calculation of the specific heat for a 24-site cluster. We show curves indicating onset of stripy SDW order at higher temperatures and the effect of the vison gap at lower temperatures. The vertical dashed line ($J/K \approx 0.12$) in Fig. 4 separates the KSL and PSL phases. Remarkably, the vison gap, a distinguishing feature of the KSL phase, extends well into the PSL phase, vanishing only at the special point $J/K = 0.5$ where the stripy SDW order peaks. The inset shows the expectation value of the Kitaev plaquette flux operator W_p – a Wilson loop – as a function of temperature, for different values of J/K . The stars on the curves indicate the position of the vison gap anomaly in the specific heat. In the Kitaev model, every state is deconfined; whence, at low temperatures the W_p take the nonzero expectation value, $\langle W_p \rangle = 1$. The introduction of Heisenberg perturbations introduces fluctuations of the Z_2 gauge fields; nevertheless we find $\langle W_p \rangle \approx 1$ throughout the KSL phase. Once inside the PSL phase, $\langle W_p \rangle$ decreases rapidly with increasing J/K but remains finite and positive all the way to $J/K = 0.5$ where it vanishes. Thus despite the appearance of stripy SDW order, the low-lying states in the PSL phase show two key features - deconfinement and vison gap - of the KSL phase. In this sense the PSL phase at low temperatures is rather reminiscent of a supersolid phase. Note that the vison gap appears at an energy scale significantly smaller than the coupling con-

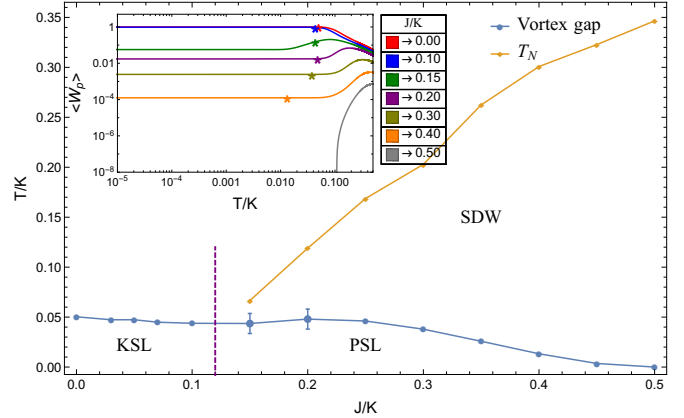


Figure 4. Finite temperature phase diagram for the $J - K$ model obtained from specific heat calculations. The vison (vortex) gap, characteristic of the KSL phase, persists well into the PSL phase, vanishing only at $J/K = 0.5$ where stripy SDW order peaks, and beyond. The PSL phase has two subdivisions, a purely stripy SDW phase at higher temperatures, and a nonzero expectation value for the plaquette Wilson loop operators, or Kitaev fluxes, (signature of the deconfined KSL phase) coexisting with SDW at lower temperatures. The inset shows the Kitaev flux expectation value W_p . The crosses in the inset curves mark the position of the specific heat anomaly associates with the vison gap. Note that the vison gap appears at a much smaller energy scale than the terms in the Hamiltonian.

stants in the Hamiltonian. At higher temperatures, the vanishing of $\langle W_p \rangle$ again indicates confinement, and only stripy SDW order survives.

To conclude, quasiparticle excitations of the Kitaev model decay when perturbed by sufficiently strong Heisenberg interactions, with stronger perturbations necessary near the ends of the excitation spectrum, and approaching zero (within numerical accuracy) at the center. Similarly analyzing the stripy SDW states, we found that over a range of J/K in the proximate spin liquid (PSL) phase, exact eigenstates at low-energies are more Kitaev-like than SDW. At sufficiently high energies, both Kitaev and stripy SDW states become unstable. In the PSL phase, for larger values J/K , the low-energy excitations may resemble stripy SDW better than Kitaev. We framed the question of quasiparticle stability in the language of a many-body localization (MBL) transition in the Fock space of exact eigenstates of the $J - K$ model. Calculation of the support sizes of Kitaev and stripy SDW states in the Fock space required a knowledge of a large number of excited states of clusters with up to 24 spins, for which the FEAST and Krylov-Schur algorithms were used. Finite temperature analysis of the specific heat and the vison (flux) gap revealed that the low temperature regime in the PSL has the characteristics of a supersolid, simultaneously showing deconfinement and density wave order.

Our findings may also be relevant to the Kitaev materials $\alpha\text{-RuCl}_3$ and Na_2IrO_3 , that are believed to be in

a PSL phase, although the ground state order is of the zigzag SDW type owing to somewhat different competing interactions. Our study suggests that probing low-energy excitations is more likely to reveal Kitaev quasiparticle effects than excited states above the zigzag SDW ordering scale. This view is supported, for example in the observation of quantized thermal Hall conductivity [42] at low temperatures in $\alpha\text{-RuCl}_3$ (but not at higher temperatures), and the field-induced quantum spin liquid state inferred from high-field magnetometry at low temperatures [49] in Na_2IrO_3 . Similarly, the incoherent features seen in inelastic neutron scattering measurements at higher energy scales [3, 43], while supporting the case that magnons may not be good quasiparticles here, do not necessarily imply that the excitations instead resemble Kitaev quasiparticles. Recent numerical studies [4] of realistic spin models for $\alpha\text{-RuCl}_3$ suggest that the ground state at intermediate magnetic fields is a Kitaev spin liquid based on the appearance of field induced Z_2 flux states. It would be interesting to make a direct comparison with the Kitaev wavefunctions in this regime.

We end with some comments on the relevance of our findings in the general context of MBL transitions. Disorder [55, 57], a common cause of MBL, is absent in our model; however, it is not strictly necessary for localization – recent developments [58–60] show that MBL transitions are also possible in disorder-free systems. A distinguishing feature of such disorder-free models is that the many-body localized and delocalized phases are both nonergodic [61]. Interestingly, we find that the level-spacing distribution remains Poisson-like in the entire parameter space (see SI), so that our model is always non-ergodic, and yet exhibits the above MBL transitions. Another feature of the MBL transition in disordered interacting systems is the presence of a mobility edge, which has not been studied in the disorder-free context in Refs. [58–61]. Our finite size scaling analysis of the support size of Kitaev quasiparticles indicates the presence of two energy scales (mobility edges) separating many-body localized, fractal and delocalized phases.

ACKNOWLEDGMENTS

We gratefully acknowledge useful discussions with S. Bhattacharjee, K. Damle, S. Kundu, T. Senthil and V. Vinokur. Special thanks to S. Biswas for bringing to our attention the FEAST eigensolver scheme. We also acknowledge support of Department of Theoretical Physics., TIFR, for computational resources, and V.T. thanks DST for a Swarnajayanti grant (No. DST/SJF/PSA- 0212012-13).

Appendix A: localization of two-vortex states in Fock space

1. Overlap of two-vortex Kitaev state with exact eigenstates of $J - K$ model

As the Heisenberg perturbation is increased, the Kitaev states begin overlapping significantly with an increasing number of exact many-body states of the $J - K$ model. Here we show how the support size of a two-vortex state, lying close to the ground state of the Kitaev model, increases with the ratio J/K . Figure 5 shows a plot of the squares of the overlap, $|a_{ki}|^2$, of a two-vortex state of the Kitaev model with exact many-body states corresponding to two different values of J/K , where $|k\rangle = \sum_i a_{ki} |i\rangle$ is the two-vortex Kitaev state and $\{|i\rangle\}$ are the exact eigenstates of the $J - K$ model. For $J/K = 0.03$, the two-vortex state has a very small support size in the Fock space, while for $J/K = 0.7$, the support size is large. Finite size scaling behaviors of the support sizes (Figure 1 in main text) tells us about the localization of these states. For $J/K = 0.03$, this two-vortex state is localized in Fock space while for $J/K = 0.7$, the state is delocalized.

2. Finite size scaling of entanglement entropy

Apart from the inverse participation ratio, we also analyzed the scaling behavior of the entanglement entropy S_k , of the k^{th} Kitaev state with the exact eigenstates, $|i\rangle$, of the $J - K$ model:

$$S_k = - \sum_{i=1}^D |a_{ki}|^2 \log_2 |a_{ki}|^2, \quad (\text{A1})$$

The entanglement entropy shows a very similar scaling behavior as that of the support size, ξ_k . In Fig. 6, we show the scaling of the entanglement entropy of the two-flux state with N for different values of J/K . In the localized regime, $J/K \lesssim 0.12$, the slope of S_k/N vs. $1/N$ is negative, while it is positive in the fractal and delocalized regimes. In the completely delocalized regime, $J/K \gtrsim 0.5$, the entropy increases linearly with N with approximately unit slope.

Appendix B: Support sizes of higher Kitaev states

Figure 7 shows that the Kitaev states with comparable energies have comparable support sizes. The flat regions correspond to nearly degenerate Kitaev states. Some rare states appear to have anomalously low support sizes - these form a small fraction of the total, and do not affect the average trend of increasing support size with energy. This justifies regarding the energy density as an appropriate parameter for describing Fock space localization of Kitaev states.

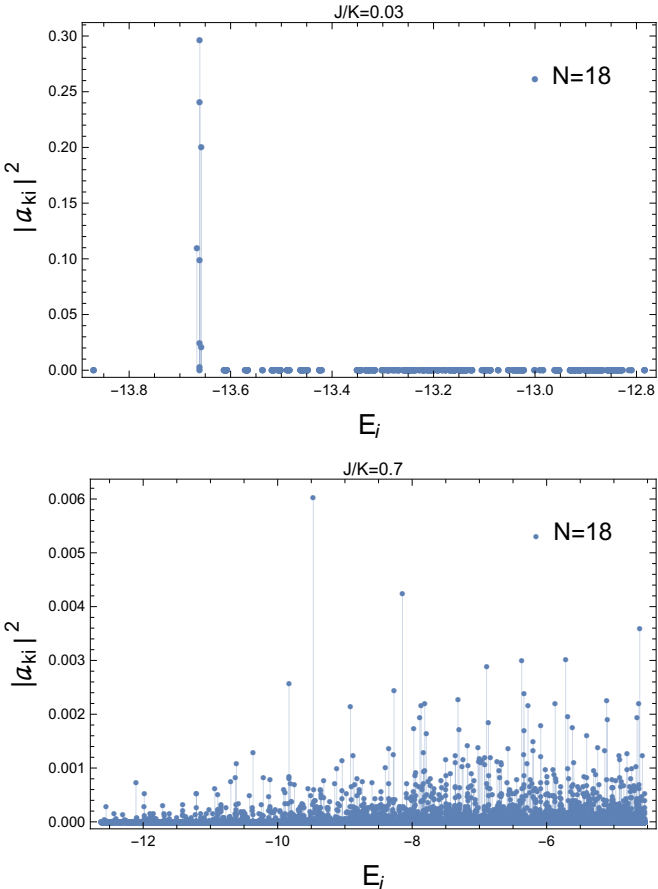


Figure 5. Plot showing the squares of the overlap of a two-vortex state of the Kitaev model with exact many-body states corresponding to two different values of J/K . The exact eigenstates are labeled by their energies. For $J/K = 0.03$, the two-vortex state has a small support size in the Fock space, and is localized, while for $J/K = 0.7$, this state is essentially delocalized. Localization and delocalization are inferred from the finite size scaling behaviors of the support sizes.

Appendix C: Energy level statistics

Figure 8 shows the distribution $P(s)$ of energy level spacings s , measured in units of the mean level spacing δ , for an 18-site cluster, for $J/K = 1$ corresponding to the fully delocalized regime for the Kitaev states. The distribution fits well to a Poisson law and not Wigner-Dyson, showing that the model is nonergodic in this fully delocalized regime. We found that the level statistics remains Poisson like throughout the localized, fractal and delocalized regimes, supporting the view[58–61] that in disorder-free models, many-body localization transitions are possible without an accompanying ergodic-nonergodic transition. For $s = 0$ (not shown in the plot), $P(s)$ takes a rather large value ~ 0.82 owing to the large number of degenerate or nearly degenerate states near the middle of the spectrum.

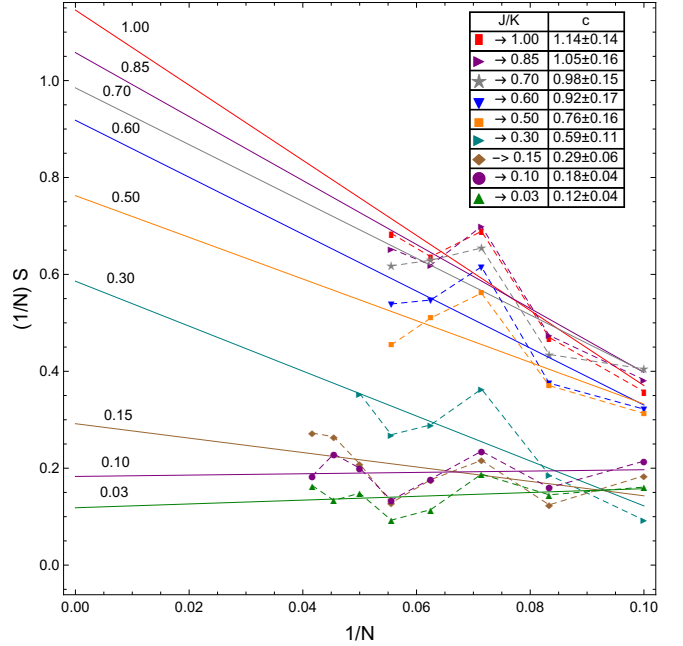


Figure 6. Plot describing finite size scaling of the entanglement entropy, S , of the lowest two-vortex Kitaev state for different values of J/K . The fits are to a volume law, $S/N = c - \frac{1}{N} \ln_2(1/f)$, where $f < 1$ and scales slower than exponential. Lines with negative (positive) slopes correspond to many-body delocalized (localized) phases. The numbers on the solid lines indicate the value of J/K .

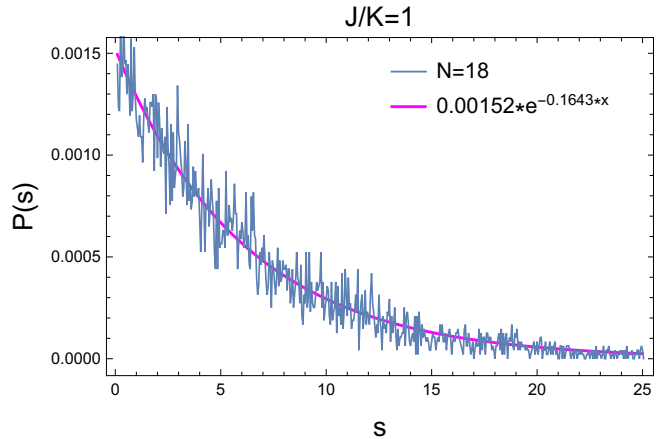


Figure 8. Plot showing the distribution $P(s)$ of energy level spacings s (in units of the mean level spacing δ) obtained for an $N = 18$ cluster, for $J/K = 1$ that corresponds to the fully delocalized regime for the Kitaev states. The fit is to a Poisson distribution, $P(s) = A \exp[-bs]$, where $A = 0.00152$ and $b = 0.16432$. The Poissonian level statistics is seen throughout the parameter space corresponding to localized, fractal and delocalized regimes. The Fock space transitions to fractal and completely delocalized phases occur completely within the nonergodic regime in our disorder-free model.

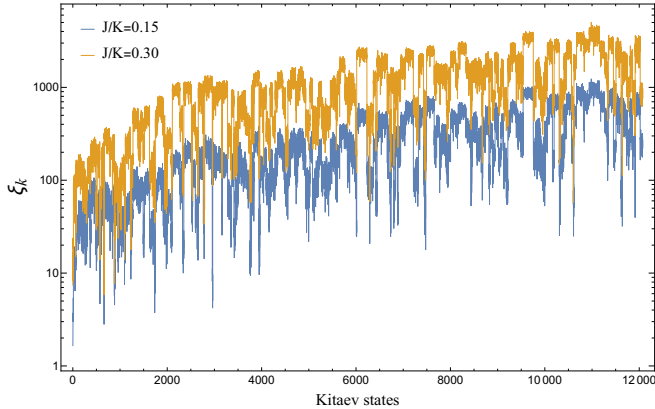


Figure 7. Figure showing the support sizes of the lowest Kitaev states in the Fock space of exact eigenstates of the $J - K$ model, for two different values of J/K . The data is for an 18-site cluster, and support sizes of the lowest 12,000 states are shown. The flat regions correspond to nearly degenerate Kitaev states. Barring some rare exceptions, Kitaev states with comparable energies have comparable support sizes. Also note the overall increase of the support size of the excited states with increasing J/K .

-
- [1] A. Kitaev, Annals Phys. **321**, 2 (2006).
- [2] M. Gohlke, R. Verresen, R. Moessner, and F. Pollmann, Phys. Rev. Lett. **119**, 157203 (2017).
- [3] S. M. Winter, K. Riedl, P. A. Maksimov, A. L. Chernyshev, A. Honecker, and R. Valentí, Nature Communications **8**, 1152 (2017).
- [4] J. S. Gordon, A. Catuneanu, E. S. Sørensen, and H.-Y. Kee, Nature Communications **10**, 2470 (2019).
- [5] J. Chaloupka, G. Jackeli, and G. Khaliullin, Phys. Rev. Lett. **105**, 027204 (2010).
- [6] I. Kimchi and Y.-Z. You, Phys. Rev. B **84**, 180407 (2011).
- [7] V. M. Katukuri, S. Nishimoto, V. Yushankhai, A. Stoyanova, H. Kandpal, S. Choi, R. Coldea, I. Rousochatzakis, L. Hozoi, and J. Van Den Brink, New Journal of Physics **16**, 013056 (2014).
- [8] Y. Sizyuk, C. Price, P. Wölfle, and N. B. Perkins, Phys. Rev. B **90**, 155126 (2014).
- [9] J. G. Rau, E. K.-H. Lee, and H.-Y. Kee, Annual Review of Condensed Matter Physics **7**, 195 (2016).
- [10] Y. Yamaji, Y. Nomura, M. Kurita, R. Arita, and M. Imada, Phys. Rev. Lett. **113**, 107201 (2014).
- [11] X. Yao, Physics Letters A **379**, 1480 (2015).
- [12] S. Bhattacharjee, S.-S. Lee, and Y. B. Kim, New Journal of Physics **14**, 073015 (2012).
- [13] K. Hu, F. Wang, and J. Feng, Phys. Rev. Lett. **115**, 167204 (2015).
- [14] H.-C. Jiang, Z.-C. Gu, X.-L. Qi, and S. Trebst, Phys. Rev. B **83**, 245104 (2011).
- [15] A. Shitade, H. Katsura, J. Kuneš, X.-L. Qi, S.-C. Zhang, and N. Nagaosa, Phys. Rev. Lett. **102**, 256403 (2009).
- [16] J. c. v. Chaloupka and G. Khaliullin, Phys. Rev. B **92**, 024413 (2015).
- [17] A. A. Vladimirov, D. Ihle, and N. M. Plakida, Journal Of Experimental And Theoretical Physics **122**, 1060 (2016).
- [18] T. Takayama, A. Kato, R. Dinnebier, J. Nuss, H. Kono, L. S. I. Veiga, G. Fabbris, D. Haskel, and H. Takagi, Phys. Rev. Lett. **114**, 077202 (2015).
- [19] H.-J. Kim, J.-H. Lee, and J.-H. Cho, Scientific Reports **4**, 5253 (2014).
- [20] J. c. v. Chaloupka, G. Jackeli, and G. Khaliullin, Phys. Rev. Lett. **110**, 097204 (2013).
- [21] R. Yadav, N. A. Bogdanov, V. M. Katukuri, S. Nishimoto, J. Van Den Brink, and L. Hozoi, Scientific reports **6**, 37925 (2016).
- [22] Z.-X. Liu and B. Normand, Phys. Rev. Lett. **120**, 187201 (2018).
- [23] K. Foyevtsova, H. O. Jeschke, I. I. Mazin, D. I. Khomskii, and R. Valentí, Phys. Rev. B **88**, 035107 (2013).
- [24] J. Knolle, G.-W. Chern, D. L. Kovrizhin, R. Moessner, and N. B. Perkins, Phys. Rev. Lett. **113**, 187201 (2014).
- [25] A. Banerjee, C. Bridges, J.-Q. Yan, A. Aczel, L. Li, M. Stone, G. Granroth, M. Lumsden, Y. Yiu, J. Knolle, et al., Nature materials **15**, 733 (2016).
- [26] S.-H. Do, S.-Y. Park, J. Yoshitake, J. Nasu, Y. Motome, Y. S. Kwon, D. Adroja, D. Voneshen, K. Kim, T.-H. Jang, et al., Nature Physics **13**, 1079 (2017).
- [27] Z. Wang, S. Reschke, D. Hünoven, S.-H. Do, K.-Y. Choi, M. Gensch, U. Nagel, T. Rö om, and A. Loidl, Phys. Rev. Lett. **119**, 227202 (2017).
- [28] Y. J. Yu, Y. Xu, K. J. Ran, J. M. Ni, Y. Y. Huang, J. H. Wang, J. S. Wen, and S. Y. Li, Phys. Rev. Lett. **120**, 067202 (2018).
- [29] Y. Singh, S. Manni, J. Reuther, T. Berlijn, R. Thomale, W. Ku, S. Trebst, and P. Gegenwart, Phys. Rev. Lett. **108**, 127203 (2012).
- [30] F. Ye, S. Chi, H. Cao, B. C. Chakoumakos, J. A. Fernandez-Baca, R. Custelcean, T. F. Qi, O. B. Korneta, and G. Cao, Phys. Rev. B **85**, 180403 (2012).

- [31] S. K. Choi, R. Coldea, A. N. Kolmogorov, T. Lancaster, I. I. Mazin, S. J. Blundell, P. G. Radaelli, Y. Singh, P. Gegenwart, K. R. Choi, S.-W. Cheong, P. J. Baker, C. Stock, and J. Taylor, Phys. Rev. Lett. **108**, 127204 (2012).
- [32] Y. Singh and P. Gegenwart, Phys. Rev. B **82**, 064412 (2010).
- [33] S. H. Chun, J.-W. Kim, J. Kim, H. Zheng, C. C. Stoumpos, C. Malliakas, J. Mitchell, K. Mehlawat, Y. Singh, Y. Choi, *et al.*, Nature Physics **11**, 462 (2015).
- [34] R. Comin, G. Levy, B. Ludbrook, Z.-H. Zhu, C. N. Veenstra, J. A. Rosen, Y. Singh, P. Gegenwart, D. Stricker, J. N. Hancock, D. van der Marel, I. S. Elfimov, and A. Damascelli, Phys. Rev. Lett. **109**, 266406 (2012).
- [35] J. P. Clancy, N. Chen, C. Y. Kim, W. F. Chen, K. W. Plumb, B. C. Jeon, T. W. Noh, and Y.-J. Kim, Phys. Rev. B **86**, 195131 (2012).
- [36] H. Gretarsson, J. P. Clancy, X. Liu, J. P. Hill, E. Bozin, Y. Singh, S. Manni, P. Gegenwart, J. Kim, A. H. Said, D. Casa, T. Gog, M. H. Upton, H.-S. Kim, J. Yu, V. M. Katukuri, L. Hozoi, J. van den Brink, and Y.-J. Kim, Phys. Rev. Lett. **110**, 076402 (2013).
- [37] H. Gretarsson, J. P. Clancy, Y. Singh, P. Gegenwart, J. P. Hill, J. Kim, M. H. Upton, A. H. Said, D. Casa, T. Gog, and Y.-J. Kim, Phys. Rev. B **87**, 220407 (2013).
- [38] X. Liu, T. Berlijn, W.-G. Yin, W. Ku, A. Tsvelik, Y.-J. Kim, H. Gretarsson, Y. Singh, P. Gegenwart, and J. P. Hill, Phys. Rev. B **83**, 220403 (2011).
- [39] K. Mehlawat, A. Thamizhavel, and Y. Singh, Phys. Rev. B **95**, 144406 (2017).
- [40] A. Banerjee, P. Lampen-Kelley, J. Knolle, C. Balz, A. A. Aczel, B. Winn, Y. Liu, D. Pajerowski, J. Yan, C. A. Bridges, *et al.*, npj Quantum Materials **3**, 8 (2018).
- [41] L. Wu, A. Little, E. E. Aldape, D. Rees, E. Thewalt, P. Lampen-Kelley, A. Banerjee, C. A. Bridges, J.-Q. Yan, D. Boone, S. Patankar, D. Goldhaber-Gordon, D. Mandrus, S. E. Nagler, E. Altman, and J. Orenstein, Phys. Rev. B **98**, 094425 (2018).
- [42] Y. Kasahara, T. Ohnishi, Y. Mizukami, O. Tanaka, S. Ma, K. Sugii, N. Kurita, H. Tanaka, J. Nasu, Y. Motome, *et al.*, Nature **559**, 227 (2018).
- [43] K. Ran, J. Wang, W. Wang, Z.-Y. Dong, X. Ren, S. Bao, S. Li, Z. Ma, Y. Gan, Y. Zhang, J. T. Park, G. Deng, S. Danilkin, S.-L. Yu, J.-X. Li, and J. Wen, Phys. Rev. Lett. **118**, 107203 (2017).
- [44] L. J. Sandilands, Y. Tian, A. A. Reijnders, H.-S. Kim, K. W. Plumb, Y.-J. Kim, H.-Y. Kee, and K. S. Burch, Phys. Rev. B **93**, 075144 (2016).
- [45] L. J. Sandilands, Y. Tian, K. W. Plumb, Y.-J. Kim, and K. S. Burch, Phys. Rev. Lett. **114**, 147201 (2015).
- [46] K. W. Plumb, J. P. Clancy, L. J. Sandilands, V. V. Shankar, Y. F. Hu, K. S. Burch, H.-Y. Kee, and Y.-J. Kim, Phys. Rev. B **90**, 041112 (2014).
- [47] G. Jackeli and G. Khaliullin, Phys. Rev. Lett. **102**, 017205 (2009).
- [48] I. A. Leahy, C. A. Pocs, P. E. Siegfried, D. Graf, S.-H. Do, K.-Y. Choi, B. Normand, and M. Lee, Phys. Rev. Lett. **118**, 187203 (2017).
- [49] S. D. Das, S. Kundu, Z. Zhu, E. Mun, R. D. McDonald, G. Li, L. Balicas, A. McCollam, G. Cao, J. G. Rau, H.-Y. Kee, V. Tripathi, and S. E. Sebastian, Phys. Rev. B **99**, 081101 (2019).
- [50] S.-H. Baek, S.-H. Do, K.-Y. Choi, Y. S. Kwon, A. U. B. Wolter, S. Nishimoto, J. van den Brink, and B. Büchner, Phys. Rev. Lett. **119**, 037201 (2017).
- [51] K. Riedl, Y. Li, S. M. Winter, and R. Valentí, Phys. Rev. Lett. **122**, 197202 (2019).
- [52] E. Polizzi, Phys. Rev. B **79**, 115112 (2009).
- [53] G. W. Stewart, SIAM Journal on Matrix Analysis and Applications **23**, 601 (2002).
- [54] S. R. White, Phys. Rev. Lett. **69**, 2863 (1992).
- [55] B. L. Altshuler, Y. Gefen, A. Kamenev, and L. S. Levitov, Phys. Rev. Lett. **78**, 2803 (1997).
- [56] The energy density is the energy per site in dimensionless units, normalized by the ground state energy scale.
- [57] A. D. Mirlin and Y. V. Fyodorov, Phys. Rev. B **56**, 13393 (1997).
- [58] A. Smith, J. Knolle, D. L. Kovrizhin, and R. Moessner, Phys. Rev. Lett. **118**, 266601 (2017).
- [59] M. Brenes, M. Dalmonte, M. Heyl, and A. Scardicchio, Phys. Rev. Lett. **120**, 030601 (2018).
- [60] M. C. Diamantini, C. A. Trugenberger, and V. M. Vinokur, Communications Physics **1**, 77 (2018).
- [61] A. Smith, J. Knolle, R. Moessner, and D. L. Kovrizhin, Phys. Rev. Lett. **119**, 176601 (2017).